Wind Energ. Sci., 10, 227–243, 2025
https://doi.org/10.5194/wes-10-227-2025

eawe european academy of wind energy
Open Access WIND ENERGY SCIENCE

Challenges in detecting wind turbine power loss: the effects of blade erosion, turbulence, and time averaging

Tahir H. Malik[1] **and Christian Bak**[2]

[1]Vattenfall, Amerigo-Vespucci-Platz 2, 20457 Hamburg, Germany
[2]DTU Wind and Energy Systems, Frederiksborgvej 399, 4000 Roskilde, Denmark

Correspondence: Tahir H. Malik (tahir.malik@vattenfall.de)

Received: 27 March 2024 – Discussion started: 4 April 2024
Revised: 28 November 2024 – Accepted: 6 December 2024 – Published: 23 January 2025

Abstract. Establishing a clear correlation between blade leading-edge erosion (LEE) and the performance of operational wind turbines is challenging due to the complex interaction of various factors. This study aims to improve the understanding and analysis of real wind turbine measurements by employing aeroelastic simulations to investigate the combined effects of LEE, turbulence intensity (TI), and time averaging as a data processing technique and to show how they obscure the effects of erosion. The study does not aim to investigate each contributing factor in detail but seeks to provide insights through selected examples, thereby illustrating how these conditions hinder the detection of blade erosion's effects on power loss. An aeroelastic model provided by an offshore original-equipment manufacturer (OEM) was used to simulate various scenarios. Turbulence intensity was varied for a range of wind speeds, and the aerofoil characteristics for the blade were modified to simulate different degrees of erosion, represented by varying levels of roughness. For a given site, findings reveal that even mild simulated erosion can reduce the annual energy production (AEP) by 0.82 % at 6 % TI, while more severe erosion leads to a 1.46 % decrease. Furthermore, increasing TI exacerbates these losses, with 15 % TI causing up to 2.14 % AEP reduction for eroded blades, making it increasingly difficult to distinguish between the effects of blade erosion and turbulence intensity on turbine performance. These effects are most pronounced at sites with lower average wind speeds. Moreover, the interaction between TI levels and longer time-averaging periods, which vary with wind speed, can obscure the true magnitude of LEE's impact on short-term power fluctuations. This study suggests that 10 min time-averaging periods can mask performance and that analysing unsteady-rotor data with shorter time periods, such as 1 s periods, is preferable. The work emphasises the importance of considering the blade condition's impact in the context of various influencing factors for accurate AEP assessments, performance monitoring, and improved wind turbine design for operational wind turbines.

1 Introduction

The performance of wind turbines is a multifaceted subject of research, being affected by a multitude of environmental (Wharton and Lundquist, 2012) and operational factors. Wind turbine manufacturers and owners place significant emphasis on this aspect due to its implications for revenue as well as for operations and maintenance (O&M). Despite this, accurately identifying and validating performance within operational wind turbines using their self-generated supervisory control and data acquisition (SCADA) measurement data remains a significant challenge (Ding et al., 2022). This challenge stems from the complex interaction of factors affecting the turbine's performance (Barthelmie and Jensen, 2010), making it difficult to isolate the effects of individual causes amidst the numerous variables and uncertainties. Consequently, extensive efforts have been invested in analysing SCADA data, with the default approach involving the analy-

sis of 10 min time-averaged values of wind speed and power, focusing particularly on power degradation over time. Nevertheless, it is acknowledged that significant uncertainties exist within this 10 min time-averaging analysis (Yang et al., 2014), complicating the detection of leading-edge erosion's (LEE's) effects. In industrial practice, operators typically calculate power curve loss contributions using static components, employing static tables that include factors such as the thrust coefficient, C_t; temperature; wind shear; transformer losses; and component friction. Yet quantifying the impact of LEE on the power curve for operating turbines remains a challenge. Despite the extensive research on individual factors such as turbulence and other environmental conditions, a comparative analysis of blade erosion's impact relative to effects such as turbulence intensity and time-averaging periods has remained unexplored for operational turbines, which the present study aims to address.

This study specifically investigates the degradation of power due to LEE. The detrimental effects of LEE or leading-edge roughness (LER) on aerofoil characteristics have been extensively documented in wind tunnel experiments (Hansen, 2008; Maniaci et al., 2016; Gaudern, 2014; Krog Kruse et al., 2021; Bak et al., 2023). Furthermore, these effects have also been the subject of numerous studies on the impact of erosion on wind turbine annual energy production (AEP; Bak et al., 2016; Ehrmann et al., 2017; Kruse, 2019; Han et al., 2018; Castorrini et al., 2023). These studies indicate potentially significant AEP losses of up to 7 %. While the impact of blade erosion on AEP is generally smaller than that of wake deficits, and some controllers can compensate for degraded lift through pitch adjustments, its subtle effects are nonetheless important to quantify. This study employs multibody simulations to capture the interaction between LEE and factors including turbulence intensity (TI) and data time averaging, providing a more quantitative understanding of how these factors obscure performance losses in SCADA data and aiming to bridge the gap in understanding. Currently, a 1 % variance in AEP for Vattenfall, an energy utility, equates to an average daily loss of approximately 380 MWh. Although the effects of LEE on aerodynamic performance are easily measurable in controlled environments such as wind tunnels, the question is not whether aerodynamic losses occur; instead, it is why these effects are obscured within the scattered sensor signals generated by operational wind turbines and how to detect them when a rotor operates in a turbulent flow field with significant wind fluctuations.

Analysis of extensive measurement data from wind farms revealed difficulties obtaining sufficient understanding of the influencing mechanisms, a finding supported by studies from Badihi et al. (2022) and Gonzalez et al. (2019). Consequently, simulations of a wind turbine within a wind farm environment were deemed necessary to complement the analysis of SCADA data. The analysis of the simulated data, again, revealed that understanding how turbulence intensity (TI) and the effect of averaging unsteady data influenced the results was crucial for interpreting both measured and simulated data. Furthermore, turbulence is a well-known atmospheric condition that significantly impacts wind turbine performance (St. Martin et al., 2016; Saint-Drenan et al., 2020; Kim et al., 2021; Cappugi et al., 2021).

This study aims to investigate selected factors that obscure the detection of erosion-induced power losses in operational wind turbines, addressing a gap in the current literature. Rather than conducting an exhaustive analysis of all potential contributors, the investigation focuses on providing insights into these obscuring effects through key examples and proposes potential mitigation strategies. While the need for further analysis is acknowledged, the objective is to illustrate how specific atmospheric conditions and analysis methods complicate the identification of blade erosion's impact on power loss. A key aspect of this work is the incorporation of a certified model of an operational turbine's controller into a full aero–servo–elastic simulation loop, which ensures that the response to degraded blades, including pitch adjustments utilising aerodynamic reserves, is captured accurately.

In this manner, the study aims to improve the understanding and analysis of wind turbine performance measurements rather than focusing on aerodynamic computations. The goal is to develop more reliable methods for detecting degradation in real-world wind turbine performance. With these aims, the study also investigates and compares significant effects, such as turbulence intensity, alongside the impact of degraded aerofoil polar coefficients (C_L and C_D), to uncover why erosion's effects are not easily detected in SCADA data. The influence of turbulence intensity is investigated at the rotor level, expanding upon existing knowledge that primarily focuses on performance at the aerofoil level (e.g. Bak et al., 2008, and Cappugi et al., 2021). Furthermore, the effects of time averaging, traditionally performed using 10 min periods, are examined.

2 Method

This study aims to conduct an investigation into the impact of turbulence intensity on the aerodynamic performance of wind turbine rotors, focusing on the effects of leading-edge erosion. This was achieved using aeroelastic code that incorporates structural dynamics. The effects of wind shear were also investigated in brief. Additionally, the study examined the potential impact of different time-averaging periods used in operational data analysis on the ability to detect and quantify the effects of leading-edge erosion.

2.1 Wind turbine and aeroelastic code

The investigation utilised the blade-element-momentum-based (BEM-based) multibody aero–servo–elastic tool HAWC2 (Horizontal Axis Wind turbine simulation Code, 2nd generation), developed by DTU Wind Denmark. A

comprehensive description of the usage and implementation of HAWC2 is well-documented in the literature (Larsen and Hansen, 2007). The certified multibody model used in this study, provided by an original-equipment manufacturer (OEM), represents a currently operational offshore wind turbine. It is a three-bladed multi-megawatt horizontal-axis wind turbine with variable speed, pitch regulation, and yaw control, with nominal power between 3 and 4 MW. The Reynolds number, Re, can be estimated using the rule of thumb from Bak (2023), which states that Re is proportional to the rotor radius, R, and ranges between $75\,000 \cdot R$ and $150\,000 \cdot R$. Consequently, Re is approximately 7 million. Due to intellectual-property considerations, specific details about the turbine, such as structural properties and control philosophy, are not disclosed; hence, the power is presented as *normalised power* and is expressed as power relative to the rated power.

While reference wind turbines such as the National Renewable Energy Laboratory (NREL) 5 MW (Jonkman et al., 2009) or the DTU 10 MW (Bak et al., 2013) could have been employed, this study's close connection to wind farm measurements necessitated incorporating a controller from an actual wind turbine to investigate unsteady effects. Since relative changes in performance are more critical than absolute performance, analysing a real wind turbine model was considered important. Various parameters, such as damage severity, radial position, and the turbine-specific power, impact potential degradation. Therefore, this study should indicate general trends, with specific numerical results likely to vary slightly depending on the actual wind turbine design.

2.2 Representing leading-edge erosion

Blade leading-edge erosion was modelled as varying levels of surface roughness, a measure of damage severity impacting aerodynamic performance and representing a precursor to more significant aerofoil deterioration where voids or cavities may begin to form. The multibody model's original blade aerofoil polars for the outer 15 % of the blade length were modified, applying factors to reflect the effects of erosion. The length and location of this applied degradation is comparable to field observations of similar blades after approximately 2 years of operation. Wind tunnel tests conducted by Krog Kruse et al. (2021) utilised P400- and P40-grit sandpaper to simulate distinct erosion levels on a National Advisory Committee for Aeronautics (NACA) 63_3-418 aerofoil. These textures, representing rain-induced erosion, provided empirical references for deriving aerofoil polar degradation factors, which were subsequently applied to the aeroelastic model to assess their effects on aerodynamic performance. It is important, however, to acknowledge that real-world degradation of turbine blade leading edges can be influenced by a multitude of factors beyond those captured in this controlled simulation.

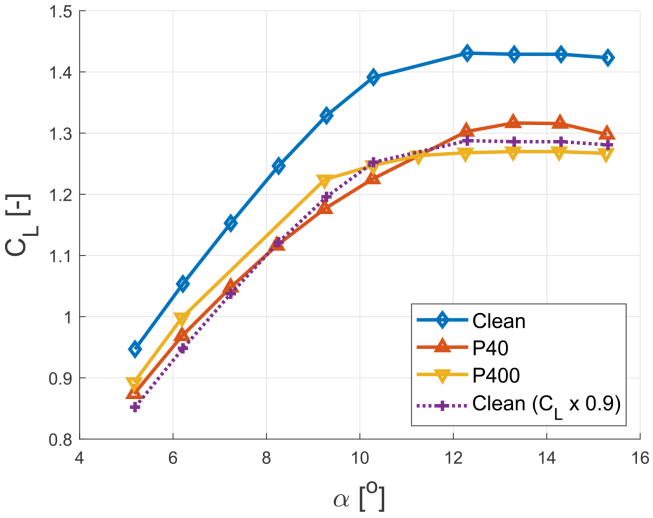

Figure 1. Effects of leading-edge erosion on the lift coefficient (C_L) as a function of the angle of attack (α). Comparing clean, P40, and P400 blade roughnesses, demonstrates decreased C_L with increased roughness (measurement data from Krog Kruse et al., 2021).

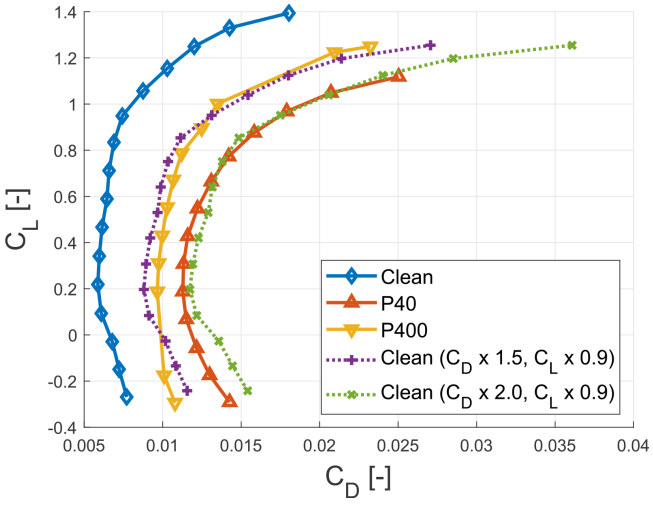

Figure 2. Effects of leading-edge erosion on the drag coefficient (C_D) as a function of the lift coefficient C_L). Comparing clean, P40, and P400 blade roughnesses, demonstrates increased C_D with increased roughness (measurement data from Krog Kruse et al., 2021).

A limitation of this work was the lack of access to the aerofoil geometry. Despite the aerofoil characteristics being available, they may not be shown due to intellectual-property rights. Therefore, the degradation of the proprietary aerofoil characteristics was modelled by applying relative changes derived from wind tunnel tests performed on an alternative aerofoil. While Skrzypinski et al. (2014) proposed a model for altering aerofoil characteristics, this study employed a different approach. Although the alternative aerofoil from which the factors were derived was not an identical match

to that in the multibody model, this method provided a suitable approximation for representing erosion on the outboard region of turbine blades.

Wind tunnel tests on the alternative aerofoil were conducted at a Reynolds number of 5×10^6. Results for the clean (no sandpaper) and the P400 (fine, with an average roughness value of 0.035 mm) and P40 (coarse, with an average roughness value of 0.415 mm) sandpaper were used. The P40 sandpaper, which has a larger grain size, was chosen to represent a more severe erosion state. Figures 1 and 2 illustrate that for both P400 and P40 sandpaper roughnesses, the C_{Lmax} is reduced by approximately 10 % within a specific range of α before deep stall. Similarly, the C_{D} increased by approximately 50 % for P400 roughness and 100 % for P40 roughness, compared to a clean aerofoil surface. These percentage changes in the lift and drag coefficients were subsequently applied to approximate the degradation of the proprietary aerofoil polars used in the simulation model. For simplicity, the lift polar representing the clean aerofoil was scaled by a factor of 0.9. Additionally, two artificial drag polars were created by scaling the drag polar representing the clean aerofoil by factors of 1.5 and 2.0.

This approach was chosen as the multibody simulations were performed over a limited range of angles of attack, which are relevant for the cases of normal turbine operation detailed in Sect. 2.5. These factors were applied between the aerofoil's minimum and maximum lift angles of attack. Beyond this range, at high angles of attack (30°), the adjusted characteristics were smoothly blended into the original data. The assumption was that at high angles of attack, the performance is dominated by the flow separation, and the resulting pressure distribution resembles that of a flat plate, thus being less dependent on the specific surface characteristics. Due to confidentiality, the final modified aerofoil characteristics may not be shown.

2.3 Representing wind farm turbulence

The simulations were designed to represent turbulence conditions typical of an operational offshore wind farm. Turbulence data were sourced from a meteorological mast located adjacent to an operational offshore wind farm that utilises the same turbine type as the multibody model.

The turbulence intensity profile at the site, corrected to the turbine's hub height using WindPro (EMD International A/S, 2023), is shown in Fig. 3. This comprehensive dataset was derived from 6 years of 10 min averaged data and included all wind speeds without directional filtering. It incorporated the effects of wakes from adjacent turbines as well as a wind farm, offering a representation of the first row in a wind farm environment.

The mean TI was 7.3 % for the entire period and 6.7 % when limited to turbine operational wind speeds – between 4 and 25 m s^{-1}. The TI distribution is depicted in Fig. 4, and together, these figures reveal that although higher turbulence

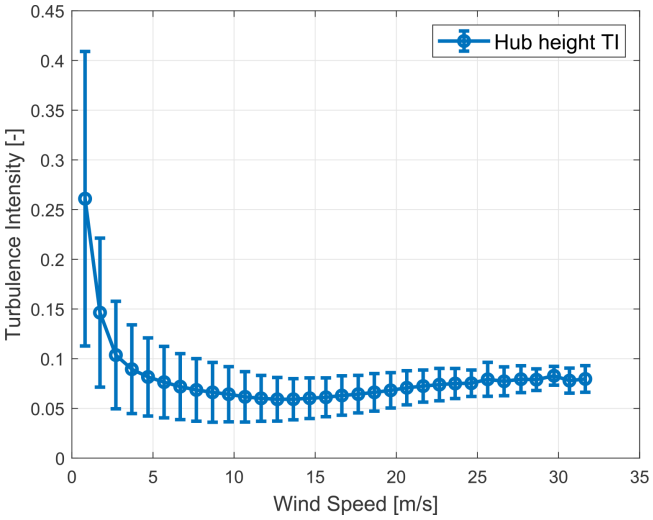

Figure 3. Turbulence intensity at the hub height as a function of wind speed. Data were obtained from the wind farm's meteorological mast.

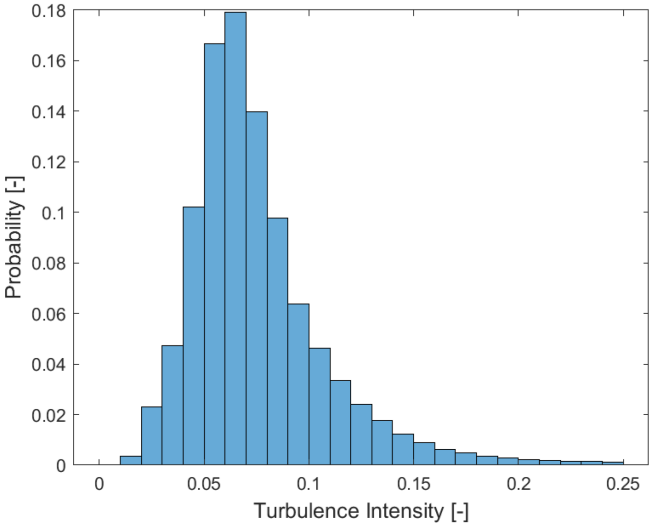

Figure 4. Probability density distribution of turbulence intensity (TI) for wind speeds between 4 and 25 m s^{-1} (limited at 25 %).

intensities did occur, they were relatively rare and primarily occurred at lower wind speeds. For sake of convenience in the simulation environment, a turbulence intensity of 6 % was used to represent mean annual wind farm turbulence with wake-free directional filters applied. Specific location details of the wind farm and the met mast are omitted due to confidentiality.

2.4 Data time averaging

To better understand the potential impact of different data processing techniques on wind and power measurements, this study investigated the effects of varying time-averaging

periods on the detection and quantification of erosion-related power losses. The analysis of wind and power measurements often involves binning and time averaging. Binning and time averaging data are forms of data filtering that can both clarify and potentially complicate the interpretation of results. Careful selection of bin sizes is crucial to avoid information loss and potential misinterpretation.

Data time averaging, traditionally over a 10 min period, is used to smooth turbine signals such as wind speed or power and behaviours such as pitch or torque. These responses are slightly delayed relative to wind speed, which can fluctuate rapidly. Time averaging can provide a more representative overview of turbine performance and prevailing wind conditions, allowing the identification of trends and patterns in data, supported by findings from Abolude and Zhou (2018), Do and Berthaut-Gerentes (2018), and Elliott and Infield (2012) that express associated benefits and complexities. While longer periods simplify data processing and reduce data storage needs, they also risk masking changes in performance and masking the subtle effects of leading-edge erosion on turbine behaviour (Gonzalez et al., 2017; Gonzalez et al., 2019).

Importantly, time averaging potentially introduces bias into data analysis. For instance, smoothing out short-term fluctuations in power output can inadvertently alter the perceived shape of the power curve, such as the location of the "knee" in the power curve. A crucial aspect to consider is the balance between the need to reduce noise in the data and the risk of masking important turbine responses. An excessively short time period may lead to noisy data, whereas a period that is too long risks over-filtering the turbine's behaviour.

Furthermore, time averaging affects the perceived inertia of the turbine. When power output is averaged over a longer time period, short-term fluctuations in power output are suppressed, potentially making the turbine appear less responsive to changes in wind speed. If the time period used for averaging significantly exceeds the characteristic response time of the turbine, the inertia of the turbine may be underestimated, and its ability to respond to changes in wind speed could be overestimated. Conversely, using a time period that is too short may amplify short-term fluctuations in power output, making data interpretation difficult because the raw data, in many cases, will be a swarm of data points. It is therefore important that the specific requirements of the analysis should ultimately dictate the selected time-averaging period.

To investigate these effects, this study explored the use of shorter time-averaging periods to potentially unravel the nuanced effects of leading-edge erosion on turbine performance, which may be masked in traditional 10 min averages. The challenge lies in selecting a period that offers sufficient detail without sacrificing clarity, ensuring that critical information about turbine performance and the impact of blade surface conditions is neither lost nor misrepresented. Data from multibody simulations with a 0.01 s time step were collected from all wind speed simulation seeds for a given turbulence intensity and blade profile. Time averaging was then applied to wind speed and turbine sensor variables, such as power for time periods of 0.01, 1, 30, 60, 120, 300, and 600 s. Subsequently, the data were averaged into 1 m s^{-1} wind speed bins, and the turbulence intensity of the original simulation seed was applied to the time periods sliced from it.

2.5 Simulation settings and test cases

This study employed a range of simulation cases using HAWC2, a blade-element-momentum-based (BEM-based) multibody aero–servo–elastic tool, to explore the impact of turbulence intensity and blade erosion on wind turbine performance. Simulations were executed for a range of turbulence intensities for the one clean and two eroded blade profiles. Individual cases were run in 1 m s^{-1} increments ranging from 4 to 25 m s^{-1}, representing the turbine's cut-in and cut-out wind speeds. Each configuration of wind speed, TI, and blade condition was represented by six individual simulation runs, or seeds, to ensure statistical robustness as per the International Electrotechnical Commission (IEC) (2019) 61400-1 standard.

The turbulence intensity was varied across a broad spectrum including 0 %, 4 %, 5.5 %, 6.0 %, 6.5 %, 7 %, 10 %, 15 %, and 20 %, with a focus on values around the observed average annual ambient TI at an offshore site, along with broader values for comparison. Each simulation was run for 900 s, with data from the last 600 s used for analysis to ensure that steady-state conditions had been reached. The time step of the simulations was 0.01 s. The wind shear was investigated for two conditions, including a zero-shear value and a power-law profile with an alpha value of 0.14. The air density was fixed at 1.225 kg m^{-3}, representative of sea-level conditions at 15 °C. The Mann turbulence parameter $\alpha\epsilon^{2/3}$ (Mann, 1994) energy level was set to its default value of 1.0. For a detailed explanation of specific parameters and settings, refer to the HAWC2 manual in Larsen and Hansen (2007) or to the International Electrotechnical Commission (IEC) (2019) 61400-1 standard.

3 Results and discussion

The simulations conducted in this study were analysed from multiple perspectives, with the results presented in four distinct sections:

- the effects of shear and blade erosion on power;
- the effects of turbulence intensity and blade erosion on power;
- the effects on annual energy production (AEP); and
- the effects of erosion, time averaging, and turbulence on the power curve.

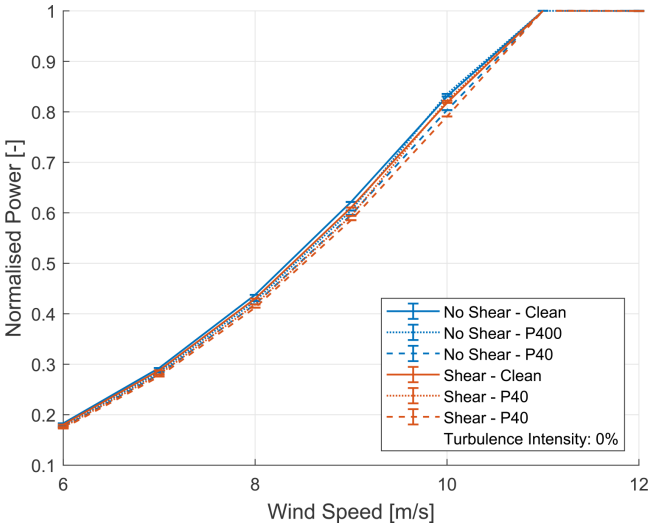

Figure 5. Effects of various blade conditions, compared to that of shear and no-shear wind conditions, on the power curve (0 % TI).

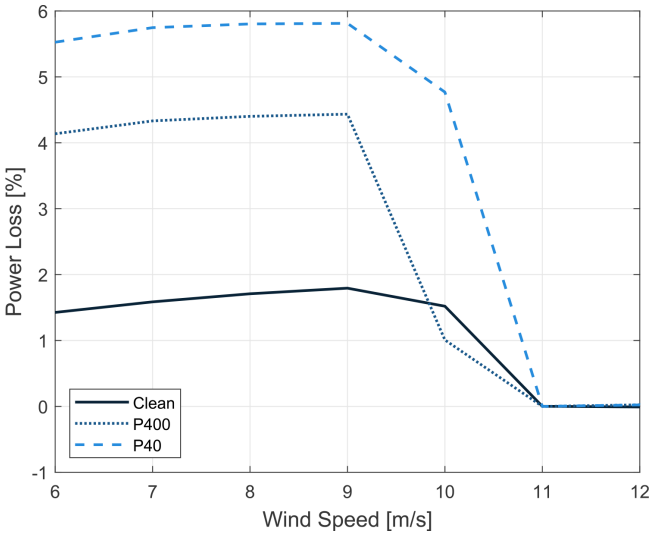

Figure 6. Percentage of power loss due to shear, referenced against the baseline clean blade without shear, for various blade conditions (0 % TI).

3.1 Effects of shear and blade erosion on power

This section examines the impact of leading-edge erosion on wind turbine power curves under different wind shear conditions using multibody simulations. The simulations were executed at a constant turbulence intensity of 0 % to isolate the distinct effects of shear and blade condition. Figure 5 presents normalised power curves for clean blades and for those exhibiting P400 and P40 roughness levels, under both zero-shear conditions and imposed wind shear conditions of a power-law profile with an alpha value of 0.14. As expected, the leading-edge roughness reduced the power output across the range of wind speeds.

Comparing the no-shear and shear conditions revealed the turbine's sensitivity to shear-induced variations in the wind profile along the rotor span. Under shear conditions, the power curves for both clean and eroded blades exhibited a shift, up to 5.8 % for the P40 roughness blade with shear, relative to a clean blade at zero-shear conditions, as seen in Fig. 6. This demonstrates an adjustment in operational behaviour to account for the velocity gradient imposed by the atmospheric shear and the convoluting effects on the power of the shear.

Despite these observed shear effects complicating the isolation of variables and highlighting the difficulty of analysing real-world measurement data, this analysis focuses on investigating turbulence, as it is an atmospheric condition whose impact on performance is typically more substantial than that of wind shear (Saint-Drenan et al., 2020). Although wind shear remains relevant, the intention is not to investigate each atmospheric condition in detail but rather to illustrate the effects through select examples.

3.2 Effects of turbulence intensity and blade erosion on power

3.2.1 Investigation based on the power curves

The normalised 10 min averaged power curve of the turbine for various turbulence intensities is shown in Fig. 7. Consistent with previous research (Saint-Drenan et al., 2020, Wagner et al., 2010), the turbine's power output is significantly influenced by turbulence intensity (TI), particularly within the partial-load region of the power curve, which represents the operational range between the wind speed where maximum rotational speed is achieved and the wind speed where rated power is reached. The plot includes higher turbulence intensities, such as 20 %, to demonstrate the trend in their effects on the power curve. This variation expresses the considerable effect of turbulence intensity on turbine performance.

A comparative analysis among clean, P400, and P40 blade conditions, representing varying degrees of erosion applied to the leading edge of the last 15 % of the blade length, is presented in Fig. 8. Results are shown for 6 % turbulence intensity, representing a typical mean value for offshore sites. The 0 % and 20 % plots are included for comparison to more outlying conditions, demonstrating a similar trend in power reduction with increasing blade erosion. A similar effect on omitted power curves affirms the consistent detrimental impact of erosion across various TI conditions.

The figures facilitate a revealing comparison of the relative effects of turbulence and erosion. Analysis of the power curve at specific points, such as the knee, reveals that changes in turbulence intensity influence power output more significantly than blade erosion does. This is evident in Fig. 8: for the clean blade at 11 $\mathrm{m\,s^{-1}}$ of wind speed, power reduces

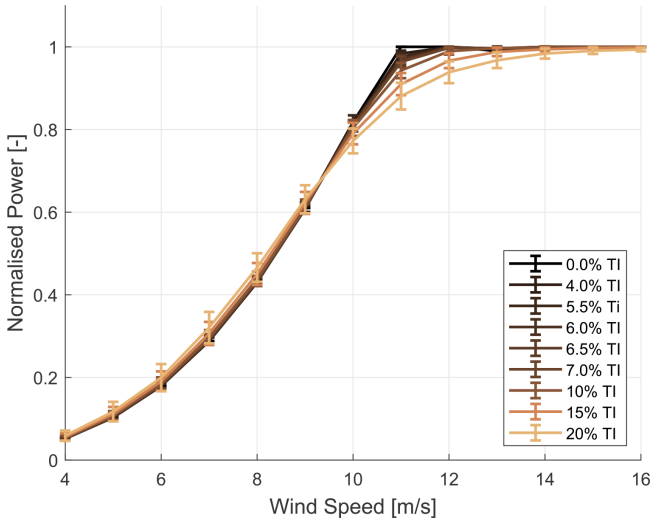

Figure 7. Effects of turbulence intensity on the power curve (clean blades).

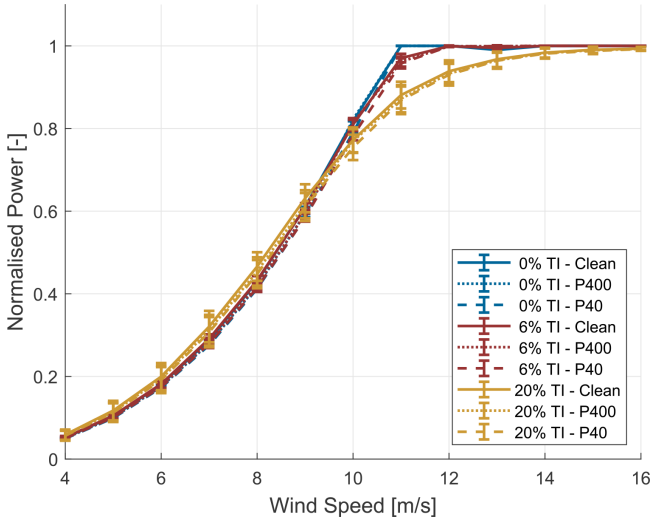

Figure 8. Effects of three specific turbulence intensities, compared to those of three blade profiles, on the power curve.

to approximately 97.0 % when TI increases from 0 % to 6 % and reduces further to 88.1 % at 20 % TI. For eroded blades, these reductions are comparable: 96.2 % and 87.2 % (P400) and 95.7 % and 86.9 % (P40).

Considering a wind speed of 11 m s^{-1} and 6 % TI, erosion causes power losses of approximately 0.9 % (P400) and 1.3 % (P40) relative to the clean blade. Importantly, the power output's standard deviation at this wind speed is approximately 1.03 % (6 % TI) and 3.23 % (20 % TI). This indicates a major challenge: particularly at higher TI, the standard deviation exceeds the power loss due to roughness, making it difficult to isolate and detect the effects of erosion on power output based on the power curve alone. Yet the comparability of values at lower TI suggests that erosion effects could potentially be detected more readily under less turbulent conditions.

An interesting observation in Fig. 8 is the intersection of power curves around 9.5 m s^{-1}. This intersection is caused by a combination of factors. Firstly, the inflection point in the power curve at 9.5 m s^{-1}, where the curvature changes, plays a role. Secondly, the averaging effects inherent to the calculation of power curves from unsteady power output contribute to this phenomenon.

While analysing the changes in power curve shapes provides valuable understanding, it offers an incomplete understanding of the true impact of erosion and turbulence. To accurately assess the overall effect, it is crucial to consider the site-specific wind speed distribution and its influence on the turbine's annual energy production. A more detailed analysis is presented in Sect. 3.3.

3.2.2 Investigation relative to a reference power curve

To further investigate how the power curve is influenced by erosion under varying turbulence intensities, this study conducted a comparative analysis. The change in power relative to a reference clean profile power curve at 6 % TI, focusing on P40 roughness, was investigated. The results are shown in Fig. 9 as a function of wind speed across a range of turbulence intensities. The delta power curve exhibits a "kink", a point characterised by a sudden change in gradient, at around 9.5 m s^{-1}, attributed to the previously discussed effect of time averaging. The most substantial reduction in power due to roughness was identified between 9 and 13 m s^{-1}. At lower turbulence intensities, i.e. 7 % and below, roughness was found to have a reducing effect on power. Moreover, for increasing turbulence intensities, the influence of roughness was amplified within the same wind speed range.

These findings highlight the non-linear and interdependent relationship between blade roughness and turbulence intensity in their impact on power output. Furthermore, they suggest that both factors must be considered when assessing wind turbine performance, especially within specific wind speed ranges.

3.2.3 Investigation using power coefficients

The coefficient of power (C_p) represents a widely used metric for evaluating the performance of wind turbines. This study analysed how C_p varies with wind speed, turbulence intensity, and blade roughness. The rationale for investigating C_p was based on the understanding that turbulence intensity does not inherently alter the efficiency of the wind turbine; rather, it is the combination of turbulence intensity and the time-averaging period that can lead to erroneous conclu-

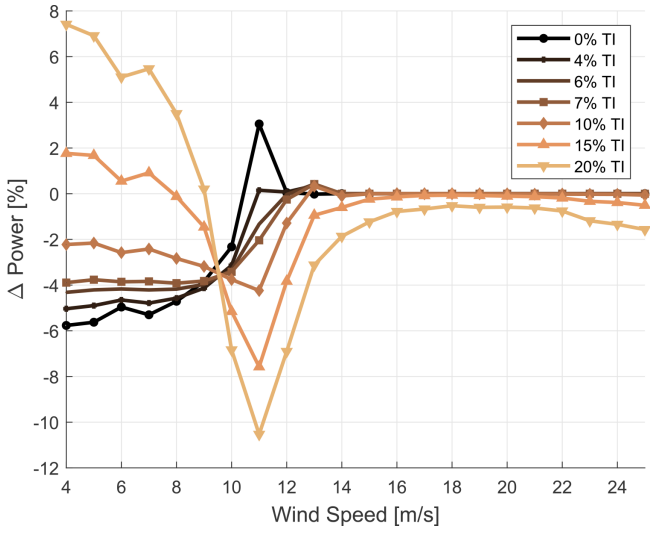

Figure 9. P40 profile – the percentage change in power output from the clean baseline as a function of wind speed, showing the impact of roughness and TI (baseline – clean profile, 6 % TI).

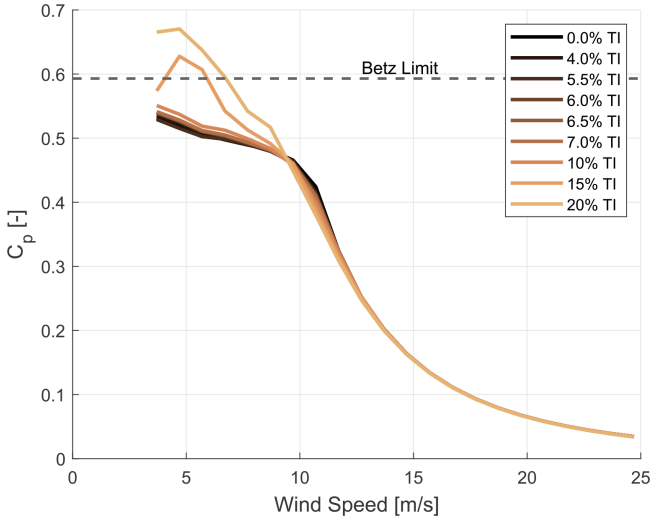

Figure 10. The power coefficient as a function of wind speed for a clean profile blade, with various turbulence intensities.

sions. The power coefficient is calculated using the following equation:

$$C_p = \frac{P}{0.5 \cdot \rho \cdot V^3 \cdot \pi \cdot R^2}, \quad (1)$$

where P is the power, ρ is the air density, V is the wind speed, and R is the rotor radius. Here, C_p is computed based on the averaged values of wind speed and power. It is important to note that the averaging was performed on wind speed and power separately before calculating C_p. This investigation also demonstrated the contrast between steady-state aerodynamic analysis with zero turbulence intensity and analysis that includes turbulence intensity. Figure 10 shows C_p as a function of wind speed for various turbulence intensities, employing a clean profile blade. The findings indicate that the most significant variation in C_p is observed at wind speeds below approximately 9 m s^{-1}. To evaluate the impact of roughened blade leading edges on C_p, Fig. 11 shows the variation in C_p for the profiles at 6 % turbulence intensity. These results suggest that the impact of both forms of roughness is less pronounced than that of a certain threshold value of turbulence intensity.

This investigation analysed multibody simulated data, focusing on the last 10 min of each simulation to capture steady-state conditions. Instances where the power coefficient (C_p) exceeded or approached the Betz limit of 0.593 in high-turbulence-intensity conditions were carefully examined. The exceeding of the Betz limit may be attributed to several factors, including turbine inertia and control dynamics, where the inherent latency in response mechanisms such as pitch and generator torque control results in a temporal mismatch between the turbine's power response and the rapid wind speed fluctuations characteristic of turbulent environments. This mismatch, particularly when results are time averaged over a 10 min window, can yield simulated C_p values that in some conditions surpass the Betz limit. Thus, it is believed that C_p values exceeding the Betz limit have no physical meaning; they are instead an artefact of the averaging of the wind speed and the rotor performance. Therefore, the analysis can lead to erroneous conclusions.

Additionally, the analysis revealed that highly turbulent conditions create localised gusts, temporarily increasing the effective wind speed at segments of the rotor, diverging from steady-state assumptions, and causing transient spikes in power output, further exacerbating the mismatch between wind speed and power output. This effect, coupled with the stochastic nature of turbulence, can enhance kinetic energy transfer to the rotor plane and momentarily boost the available wind energy beyond typical averages used in Betz limit calculations. These findings underscore the limitations of steady-state assumptions in accurately capturing the dynamic interactions between wind turbines and complex wind fields. Future research should focus on sophisticated simulation models and on analysis techniques designed to address these limitations.

Figure 12 provides a further understanding of the combined effects of roughness and turbulence intensity. It depicts C_p for a limited range of lower turbulence intensities, along with the three blade profiles at 6 % TI for wind speeds up to 11 m s^{-1}. The overlap between the C_p's for turbulence intensity and roughness suggests that distinguishing between these two effects may be challenging due to the "masking" effect, particularly in high-turbulence conditions. This complicates the interpretation of aerodynamic performance degradation caused by blade erosion.

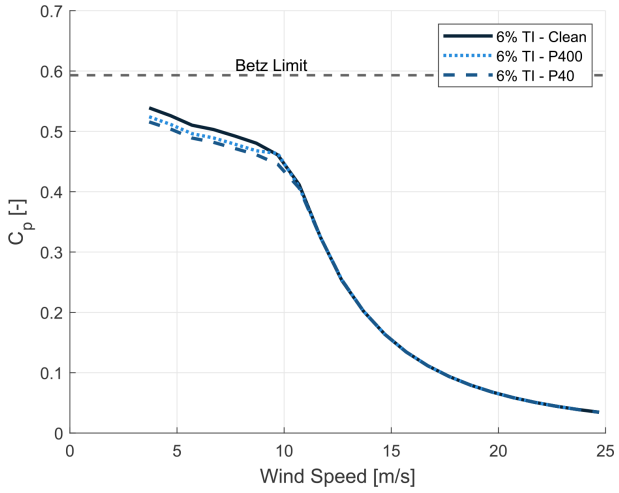

Figure 11. The power coefficient as a function of wind speed for three leading-edge profiles (6 % TI).

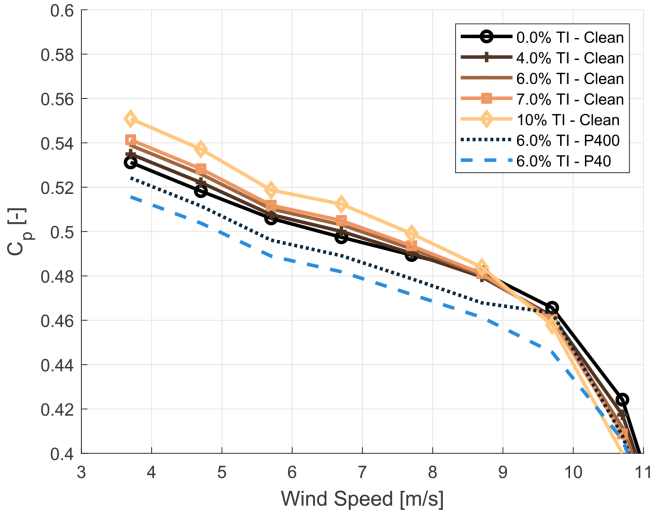

Figure 12. The power coefficient as a function of wind speed for a clean profile blade at various turbulence intensities and various leading-edge roughness profiles at 6 % TI.

3.2.4 Summary of the influence of TI and erosion on power

The findings presented herein confirm the notion that both turbulence and blade erosion exert significant influences on the wind turbine power output. It has been observed that turbulence significantly affects the power curve, predominantly in the partial-load region. Although analysing wind turbine performance under turbulent conditions is complex, this study emphasises the significance of incorporating TI in performance evaluations. This alignment with preceding studies (Wagner et al., 2010, and Saint-Drenan et al., 2020) further highlights the importance of TI in such analyses.

The examination of delta power shows the detrimental effects that blade erosion has on wind turbine power output, with the most significant power reduction due to roughness observed at wind speeds between 9 and 13 $\mathrm{m\,s^{-1}}$. This observation is consistent with prior research (Bak et al., 2020), emphasising the importance of considering roughness effects when assessing wind turbine performance. The study also showed that the impact of roughness on power output is further amplified at higher turbulence intensities, suggesting that both turbulence and erosion should be considered in performance assessment.

While the analysis focused on the impact of blade erosion on power, it is important to recognise that erosion could also influence other aspects, such as loads and sensor output. These potential impacts warrant further investigation.

3.3 Annual energy production (AEP) calculation

This section explores the calculation of annual energy production, investigating the impacts of both blade erosion and turbulence on wind turbine performance. Analyses included a real-world operational offshore wind farm and hypothetical scenarios at three fictitious sites.

3.3.1 AEP for an existing site

AEP was calculated for a wind turbine situated in an offshore wind farm operating under mean turbulence intensity of 6 %, characterised by a Weibull distribution with a scale parameter $A = 10.72$ and a shape parameter of $k = 2.17$. This corresponds to an average wind speed of 9.49 $\mathrm{m\,s^{-1}}$. The computations excluded the wake effects of upstream wind turbines.

The comparative analysis focused on quantifying the impacts of blade erosion and turbulence intensity on AEP by comparing the outcomes for three distinct blade profiles. Table 1 shows the AEP variation for each profile relative to the 6 % TI power curve of the corresponding profile.

Similarly, Table 2 shows the AEP variation for each profile relative to the clean blade profile's 6 % TI power curve. The results indicate that even mild simulated erosion, represented by the P400 blade profile, had a significant impact on the turbine's AEP, with a 0.82 % decrease. As erosion progressed, the AEP decreased further to 1.46 % for the rougher P40 sandpaper, relative to a clean blade. Moreover, once a blade is rough, its impact on AEP relative to the clean blade profile is significant.

Table 2 also presents the impact of turbulence intensities on AEP. As turbulence intensity increased, the AEP decreased for all blade profiles. The impact was more pronounced for the rougher blade profiles, with the P40 sandpaper profile already showing a strong decrease in AEP (2.14 %) for 15 % turbulence intensity.

Table 1. Changes in AEP as a function of TI. Row 2 shows the AEP change relative to clean performance at TI = 6 %. Row 3 shows the AEP change relative to P400 performance at TI = 6 %. Row 4 shows the AEP change relative to P40 performance at TI = 6 %, with $V_{ave} = 9.49\,m\,s^{-1}$ for all rows.

	TI [%]							
Blade profile	0	4	5.5	6	6.5	7	10	15
Clean delta AEP [%]	0.34	0.11	0.03	0	−0.02	−0.04	−0.23	−0.63
P400 delta AEP [%]	0.44	0.11	0.05	0	−0.04	−0.07	−0.29	−0.78
P40 delta AEP [%]	0.51	0.12	0.05	0	−0.04	−0.06	−0.26	−0.70

Table 2. Changes in the AEP as a function of TI and roughness level: the AEP change relative to clean performance at TI = 6 %, with $V_{ave} = 9.49\,m\,s^{-1}$.

	TI [%]							
Blade profile	0	4	5.5	6	6.5	7	10	15
Clean delta AEP [%]	0.34	0.11	0.03	0	−0.02	−0.04	−0.23	−0.63
P400 delta AEP [%]	−0.38	−0.71	−0.77	−0.82	−0.86	−0.89	−1.10	−1.59
P40 delta AEP [%]	−0.96	−1.33	−1.41	−1.46	−1.49	−1.51	−1.71	−2.14

3.3.2 AEP for three fictitious sites with varying wind speeds

The investigation extended AEP calculations to three hypothetical sites, each characterised by average wind speeds of 6, 8, and $10\,m\,s^{-1}$. The subsequent AEP variations for each blade profile, relative to the clean blade profile's 6 % TI power curve, are presented in Table 3 for an average wind speed of $6\,m\,s^{-1}$, Table 4 for an average wind speed of $8\,m\,s^{-1}$, and Table 5 for an average wind speed of $10\,m\,s^{-1}$. Three different climates were investigated:

- an average wind speed of $6\,m\,s^{-1}$, with $k = 2$ and $A = 6.8\,m\,s^{-1}$ (Table 3);
- an average wind speed of $8\,m\,s^{-1}$, with $k = 2$ and $A = 9.8\,m\,s^{-1}$ (Table 4); and
- an average wind speed of $10\,m\,s^{-1}$, with $k = 2$ and $A = 11.3\,m\,s^{-1}$ (Table 5).

From these results it may be concluded that the impact of turbulence intensity on AEP is more pronounced at lower average wind speeds. This observation is evidenced by the greater AEP reductions observed at lower TI levels for the P400 and P40 blade profiles, as well as the higher AEP decrease at higher TI levels for the clean blade profile at lower average wind speeds.

Concurrently, the impact of blade erosion on AEP is more significant for lower average wind speeds. This is evident from the larger AEP decrease due to blade erosion for the P400 and P40 blade profiles, as well as the higher AEP decrease for the clean blade profile at higher average wind speeds.

The large loss due to erosion for $V_{ave} = 6\,m\,s^{-1}$ is due to the fact that much of the energy is produced below rated power, where erosion has a more noticeable impact. Erosion has a negligible impact at rated power. Smaller losses due to erosion are seen for $V_{ave} = 10\,m\,s^{-1}$. The higher the TI, the greater the gain when most of the production occurs at low wind speeds, as power increases below $9.5\,m\,s^{-1}$ due to the averaging. Conversely, the higher the TI, the greater the loss when most of the production occurs at high wind speeds, as the power decreases above $9.5\,m\,s^{-1}$.

Also a trend emerges, suggesting that the comparative effects of blade erosion and turbulence intensity on AEP vary contingent upon the average wind speed and the specific blade profile under consideration. For instance, at an average wind speed of $6\,m\,s^{-1}$, blade erosion has a larger impact on AEP than turbulence intensity for all blade profiles. At higher wind speeds, turbulence intensity exerts a greater influence on AEP, particularly evident in the case of the P40 blade profile.

3.3.3 Summary of the effects of TI and erosion on AEP

The investigation into annual energy production encompassed both

- a specific actual wind climate and
- three artificial wind climates.

For the first AEP calculation, the AEP variation for the three blade profiles pertaining to a specific climate with a mean wind speed of $9.49\,m\,s^{-1}$ revealed that even minimal simulated erosion, represented by the P400 blade profile, could precipitate a notable reduction in AEP, by 0.82 %. As erosion progressed, the AEP decreased further to 1.46 % for the coarser P40 sandpaper, relative to a clean blade. Further-

Table 3. Changes in the AEP as a function of TI and roughness level: the AEP change relative to clean performance at TI = 6 %, with $V_{ave} = 6\,m\,s^{-1}$.

	TI [%]							
Blade profile	0	4	5.5	6	6.5	7	10	15
Clean delta AEP [%]	0.16	−0.04	−0.20	0	0.02	0.05	0.25	0.86
P400 delta AEP [%]	−1.20	−1.49	−1.65	−1.47	−1.46	−1.44	−1.28	−0.76
P40 delta AEP [%]	−2.51	−2.84	−3.02	−2.83	−2.82	−2.79	−2.60	−2.00

Table 4. Changes in the AEP as a function of TI and roughness level: the AEP change relative to clean performance at TI = 6 %, with $V_{ave} = 8\,m\,s^{-1}$.

	TI [%]							
Blade profile	0	4	5.5	6	6.5	7	10	15
Clean delta AEP [%]	0.32	0.08	−0.02	0	−0.01	−0.03	−0.13	−0.31
P400 delta AEP [%]	−0.51	−0.85	−0.94	−0.94	−0.97	−1	−1.13	−1.40
P40 delta AEP [%]	−1.39	−1.78	−1.89	−1.88	−1.91	−1.92	−2.03	−2.24

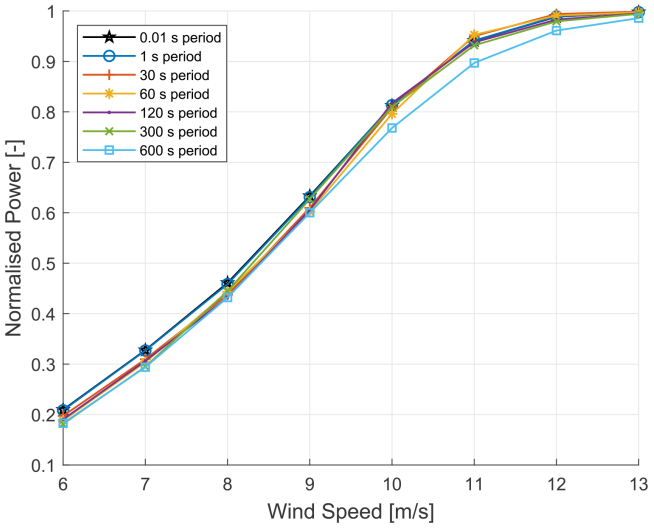

Figure 13. Clean profile – normalised power as a function of wind speed for multiple time-averaging periods, showing the impact of time periods (baseline – clean profile, 0.01 s period, 15 % TI).

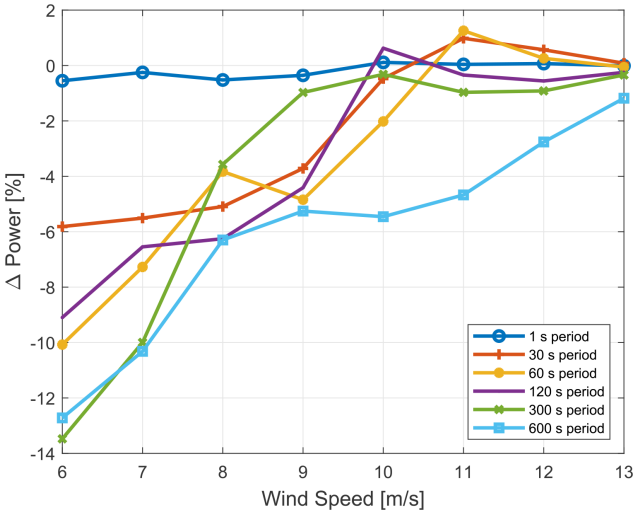

Figure 14. Clean profile – the percentage change in power output as a function of wind speed for multiple time-averaging periods, showing the impact of time periods (baseline – clean profile, 0.01 s period, 15 % TI).

more, the effect of a blade's roughness on AEP in comparison to the clean blade profile was substantial.

The second study additionally examined how three different site-specific mean average wind speeds (6, 8, and 10 m s^{-1}) affected AEP for the three blade profiles. The findings indicate that at lower wind speeds, the AEP variation caused by turbulence intensity in comparison to a clean blade profile is more important. This result shows the importance of considering the level of turbulence intensity and its impact on AEP for wind farm site selection and design considerations. Notably, the findings from the hypothetical scenario with the highest wind speed at 10 m s^{-1} corresponded well to the first AEP calculation for the specific wind climate.

From the study, it was observed that alterations in TI invariably influence AEP. Such variability introduces complexities in accurately attributing changes in AEP solely to erosion, as fluctuations in TI could equally account for observed variations.

Table 5. Changes in the AEP as a function of TI and roughness level: the AEP change relative to clean performance at TI = 6 %, with V_{ave}=10 m s^{-1}.

	TI [%]							
Blade profile	0	4	5.5	6	6.5	7	10	15
Clean delta AEP [%]	0.30	0.10	0.03	0	−0.02	−0.04	−0.21	−0.61
P400 delta AEP [%]	−0.67	−0.96	−1.02	−1.06	−1.10	−1.13	−1.32	−1.80
P40 delta AEP [%]	−0.84	−1.18	−1.25	−1.29	−1.32	−1.34	−1.52	−1.95

3.4 Influence of erosion, data time averaging, and turbulence intensity on the power curve

This section examines how blade erosion, data time-averaging periods, and turbulence intensity affect wind turbine power curves. Simulations were conducted employing both clean and eroded (P40 roughness) blade profiles.

Impact of time-averaging periods from a baseline of a 0.01 s time period at 15 % TI

Figure 13 illustrates power as a function of wind speed for different time-averaging periods at a fixed turbulence intensity of 15 %. This fixed turbulence intensity was chosen as the baseline to demonstrate only the impact of time-averaging periods at various wind speeds on the power output. The graph focuses on both the low-speed region and the knee of the power curve to highlight the varied impacts of time averaging across different wind speeds. To quantify these effects, Fig. 14 presents the percentage change in power relative to the baseline case (clean profile, 0.01 s period, fixed 15 % TI). This visualisation demonstrates the deviations in power output across various averaging periods, especially at lower wind speeds. Using a fixed turbulence intensity as the baseline, the 15 % TI example demonstrated significant reductions in observed power with longer averaging periods, with shorter time periods showing lower deviations. Notably, the 1 s period exhibited a more neutral impact on power deviation across the range of wind speeds.

Impact of time-averaging periods from a baseline of a 0.01 s time period with matched TI

To further investigate time averaging's effects, a baseline case with a clean profile and a 0.01 s period was used, with the turbulence intensity of the baseline adjusted to match that of the point analysed. The percentage difference in power from the baseline case was calculated for various turbulence intensities for a set of time-averaging periods, as illustrated in Fig. 15, showing the results for a fixed wind speed of 7 m s^{-1}, representing the low-speed region of the power curve. The data indicated the impacts of time periods as follows:

- The 1 s time period showed only a marginal effect.

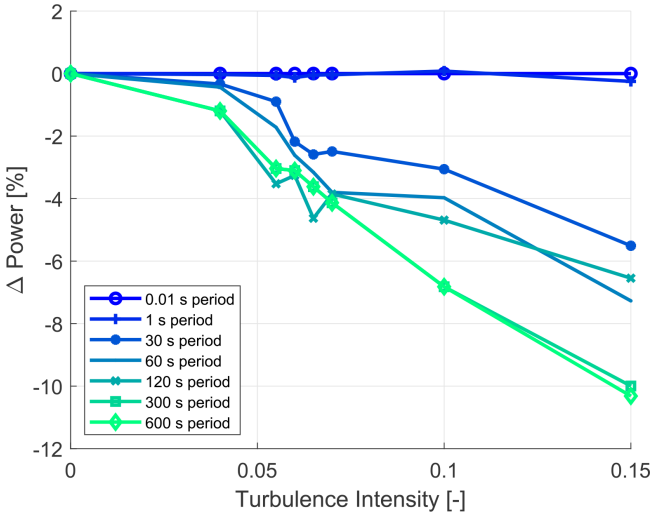

Figure 15. The 7 m s^{-1} clean profile – the percentage change in power output from the 0.01 s baseline as a function of turbulence intensity, showing the impact of time periods (baseline – clean profile, 0.01 s period, matched TI).

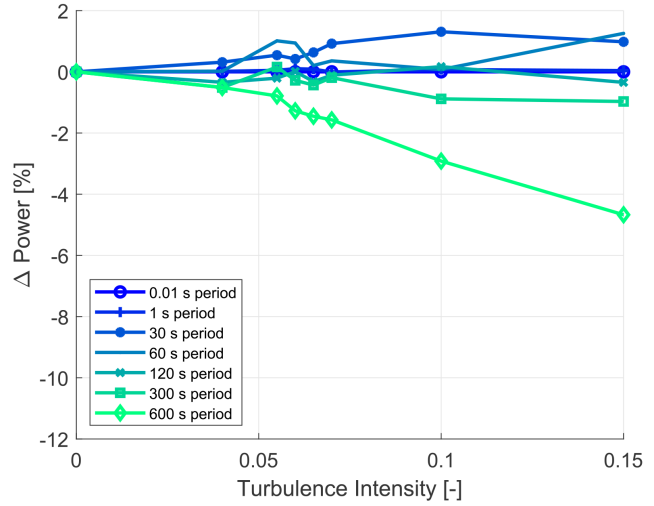

Figure 16. The 11 m s^{-1} clean profile – the percentage change in power output from the 0.01 s baseline as a function of turbulence intensity, showing the impact of time periods (baseline – clean profile, 0.01 s period, matched TI).

– There was a trend of increasing power reduction with increasing turbulence intensity.

– Longer time periods resulted in greater percentage decreases in power.

In contrast, Fig. 16 presents the results for a fixed wind speed of 11 m s^{-1}, which corresponds to the knee of the power curve. The following observations are made:

– Different time periods exhibit both increasing and decreasing effects on power output.

– Shorter time periods (30 and 60 s) pull the power curve upward.

– Periods of 1 s and 120 s have a more neutral effect.

– Increasing turbulence intensity has an approximately linear influence on power change.

In both cases, longer time periods generally showed higher delta power than shorter periods. Still, the magnitude of the change appeared larger for the 7 m s^{-1} wind speed, indicating a potentially greater impact of time periods on power output for lower wind speeds. These findings highlight the complex interaction between time-averaging periods at various turbulence intensities for two wind speeds, emphasising the need to consider these factors when analysing wind turbine power performance.

Impacts of erosion, time averaging, and turbulence from a baseline of a clean blade and fixed 0 % TI

To assess the combined effects of time averaging and turbulence as well as to compare their impacts, first a clean blade (i.e. no erosion) profile's impact on power was analysed from a baseline case of a clean profile at a 0.01 s period and, unlike in the previous two cases, with fixed 0 % TI. The impact on power for various time periods at various turbulence intensities is presented in Figs. 17 and 18. Note that erosion was not yet considered. The following points were observed:

– Again, the 1 s time period has a minimal distorting effect for all turbulence intensities and both wind speeds.

– At 7 m s^{-1}, the effect of 15 % TI is up to an 18 % increase in power for the 0.01 and 1 s time periods.

– At 7 m s^{-1}, looking at the combined effects of time averaging and turbulence, at 15 % TI the effects have a 6.5 % power increasing effect for the 600 s time period.

– At 11 m s^{-1}, the effect of 15 % TI is an up to an approximately 4.7 % decrease in power for the 0.01 and 1 s time periods.

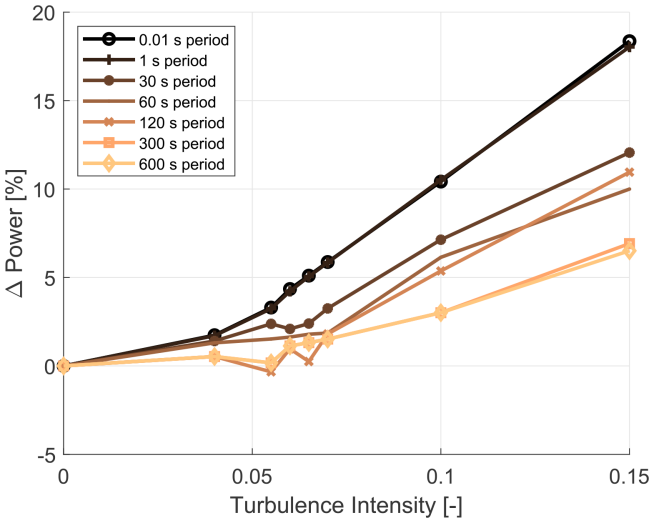

Figure 17. The 7 m s^{-1} clean profile – the percentage change in power output from the 0.01 s baseline as a function of turbulence intensity, showing the impact of time averaging and TI (baseline – clean profile, 0.01 s period, 0 % TI).

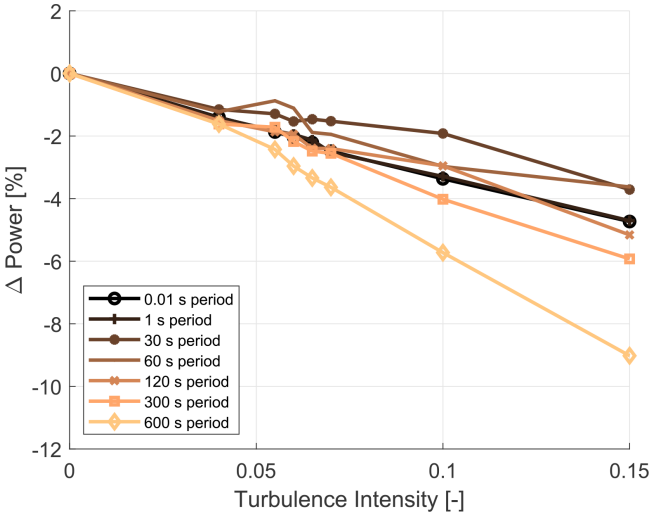

Figure 18. The 11 m s^{-1} clean profile – the percentage change in power output from the 0.01 s baseline as a function of turbulence intensity, showing the impact of time averaging and TI (baseline – clean profile, 0.01 s period, 0 % TI).

– At 11 m s^{-1}, looking at the combined effects of time averaging and turbulence, at 15 % TI the effects have an approximately 9 % power decreasing effect for the 600 s time period.

Adding the dimension of blade erosion, represented by a P40 roughness, which is of particular importance to this study, Figs. 19 and 20 display results for erosion's influence in addition to time averaging and turbulence. The baseline remained the clean blade with a 0.01 s period and fixed 0 % TI.

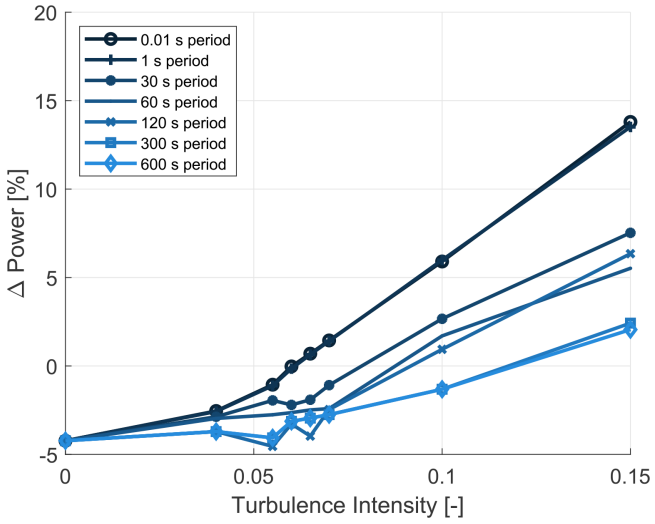

Figure 19. The 7 m s^{-1} P40 profile – the percentage change in power output from the 0.01 s baseline as a function of turbulence intensity, showing the impact of roughness, time averaging, and TI (baseline – clean profile, 0.01 s period, 0 % TI).

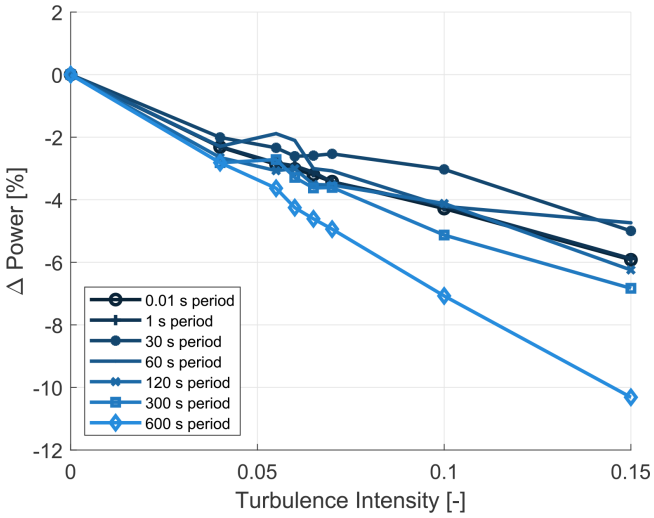

Figure 20. The 11 m s^{-1} P40 profile – the percentage change in power output from the 0.01 s baseline as a function of turbulence intensity, showing the impact of roughness, time averaging, and TI (baseline – clean profile, 0.01 s period, 0 % TI).

With the additional aspect of erosion, the following points were observed:

- The 1 s time period has a negligible distorting effect for all turbulence intensities and both wind speeds, despite blade erosion.
- At 7 m s^{-1}, the erosion, in general, reduces the power across all turbulence intensities, with an approximately 4 % power reduction observed at 0 % turbulence intensity and with a shift when compared to Fig. 17.
- At 11 m s^{-1}, the impact of erosion on power output was less pronounced compared to the lower wind speeds.

These findings emphasise the need to choose appropriate time periods for data analysis. Short periods can introduce noise, while long periods can mask important turbine behaviour. The 1 s period balances reducing variability without losing significant information. It is important to note that the effect of time averaging on power output varies with wind speed and turbulence intensity, precluding a universal correction. For accurate correction, it would be important to use both a turbine simulation model and meteorological mast data for precise TI measurements when correcting for time-averaging influences.

3.4.1 Summary of the influence of time averaging on the power curve

The investigation into time-averaging effects on power analysis showed the significant impact of time period selection on the resulting power curve. Simulation outcomes revealed that longer time periods generally lead to a more pronounced decrease in power output with increasing turbulence intensity. Despite this, the impact of time averaging on power output varies with operational conditions. At lower wind speeds, longer periods result in a significant power decrease, while at higher wind speeds, shorter periods can increase power output, and longer time periods can decrease it. Notably, a 1 s time period maintained a neutral effect across all turbulence intensities.

Comparing the P40 roughness blade to a clean blade at 0 % turbulence intensity demonstrated that the blade surface roughness's impact on power output is less pronounced than time averaging, although both factors significantly affect the power curve. Time averaging can obscure changes in wind turbine performance due to subtle aerodynamic efficiency modifications, such as blade erosion. Short-term changes are harder to detect because averaging smooths out fluctuations in the turbine's response to changes in wind speed and other variables.

To address this issue, selecting shorter averaging periods may be beneficial to capture transient variations in turbine performance. Although shorter periods may produce noisier data, this trade-off may be acceptable for detailed analysis. The study discerned minimal information loss with 1 s values, and generally, shorter periods led to smaller losses. While simulations provide good signal control, applying short averaging periods to measured data presents additional challenges due to greater uncertainties in real-world measurements.

It may be argued that the standard deviation of average values can compensate for the effect of time averaging. The standard deviation of average values can partially offset time-averaging effects by estimating lost short-term vari-

ability. Nevertheless, if the averaging period exceeds sensor response times significantly, this loss cannot be fully compensated by standard deviation calculations.

3.5 Influence of other factors

Although the current investigation demonstrates the significant impacts of blade surface roughness, turbulence intensity, and time averaging on wind turbine power output, it is important to acknowledge that additional variables also contribute. Among these variables, atmospheric conditions - including shear, as briefly demonstrated in this paper to significantly influence performance - along with temperature, veer, seasonal effects, and climate change, play pivotal roles. Changes in temperature can affect the viscosity of oils and greases, as well as lead to variations in component losses – for instance those in generators and cables – and to component stiffness. Other mechanical factors such as component wear, yaw misalignment, pitch system reliability, ageing, operations and maintenance events, and increased friction in the drive train significantly influence turbine performance. Moreover, reliable measures of wind speed, necessitating regular calibration of the turbine's wind speed sensor based on turbine output, the turbine control programmable logic controller (PLC) parameter, or software updates, along with the effects of wind speed binning, are essential to evaluate turbine performance accurately. Furthermore, the control of the wind turbine, such as generator speed and pitch as a function of wind speed or power, potentially influences the outcomes of such analyses.

Although, these aspects were outside the purview of the present study, they warrant further exploration for a comprehensive understanding of their individual and combined impacts on turbine power output. Future research, building on work such as Malik and Bak (2024), should prioritise a comprehensive approach to systematically investigate the complex interaction between these factors and their implications for the long-term efficiency and sustainability of wind turbines.

4 Conclusions

This study has examined the power and energy losses of multi-megawatt wind turbines caused by erosion-induced degradation of blade leading edges, emphasising the critical role of aerodynamic performance in wind energy capture. A significant aspect of this work has been the use of time-dependent aeroelastic computations to investigate the feasibility of observing the power degradation in real-world measurements. To achieve this, not only were the aerodynamic characteristics degraded, but the influence of turbulence intensity and the time-period for averaging data were also investigated due to their suspected influence on the analysis.

The investigation reveals that blade roughness significantly affects wind turbine performance, yet it also demonstrates that turbulence intensity significantly masks this degradation. Based on 10 min averaged data, the impact of turbulence intensity on the power is significant, especially in the partial-load region, whereas the impact of blade erosion in this region is less pronounced. Notably, blade roughness can significantly affect power production, particularly at wind speeds between 9 and 13 $\mathrm{m\,s^{-1}}$, i.e. in the transition between the partial-load region and rated power.

The power coefficient study emphasises the criticality of considering both blade roughness and turbulence intensity when assessing wind turbine performance. It appears that turbulence intensities greater than approximately 10 % make the analysis very challenging. The determination of power coefficients and the observation of values exceeding the Betz limit illustrate this.

Findings of the AEP analysis reveal that for a given site, even mild simulated erosion reduces AEP by 0.82 % at 6 % TI, while more severe erosion leads to a 1.46 % decrease. Additionally, the study indicates the variable impacts of erosion and turbulence intensity across different wind climates. In climates characterised by lower average wind speeds, the effects of erosion and turbulence intensity on AEP are accentuated compared to those in wind climates with a higher average wind speed. A key finding from this analysis is that turbulence intensities exceeding 10 % may introduce significant uncertainties in power performance analysis. Therefore, when feasible, filtering out such high-turbulence-intensity data is recommended to ensure more reliable assessment of wind turbine performance.

Furthermore, the exploration of the influence of time averaging on power output through simulations across different turbulence intensities and time periods provides additional observations. The findings indicate that longer time-averaging periods generally result in greater percentage decreases in power, where rising turbulence intensity causes a decrease in power up to approximately 10 % for 300 and 600 s periods at 15 % TI and 7 $\mathrm{m\,s^{-1}}$ wind speed. At the knee of the power curve at 11 $\mathrm{m\,s^{-1}}$, shorter time periods of 30 and 60 s elevate the power curve, while shorter time periods of 1 and 120 s have a more neutral effect. Longer time periods of 300 and 600 s lower the power curve by up to −4.5 % for the latter period at 15 % TI – although it should be noted that higher turbulence intensities are less likely at increased wind speeds. Thus, at 11 $\mathrm{m\,s^{-1}}$, different time periods have both increasing and decreasing effects on power output. This analysis has shown that 10 min (600 s) time-averaging periods result in values significantly different from those based on shorter time-averaging periods. Notably, the analysis based on 1 s time periods appears to be neutral to turbulence intensities. Thus, this study indicates that using short time periods results in less influence from turbulence intensity when analysing measurement data.

This study advances the identification of degradation in operational wind turbine measurement data, although many uncertainties remain. Future research could broaden the scope to investigate how leading-edge roughness, turbulence

intensity, wind shear, seasonal effects, yaw misalignment, and other factors such as operations and maintenance events collectively influence annual energy production. This research could focus on the long-term implications of these combined effects, potentially informing the development of optimised maintenance and operational performance monitoring strategies.

Code availability. The software code used in this study is not publicly accessible due to proprietary restrictions and confidentiality agreements, but some parts can be made available upon reasonable request to the authors. Despite this, the methodology and algorithms are described in detail within the paper, allowing readers to replicate the results. For third-party code utilised in this study, references have been provided.

Data availability. The datasets analysed in this research are not publicly accessible due to proprietary restrictions and confidentiality agreements, but some parts can be made available upon reasonable request to the authors. Nonetheless, a comprehensive description of the data methods within the paper has been provided to enable replication by interested researchers.

Author contributions. THM was the primary researcher, responsible for the conceptualisation of the study, all experimental work, data collection, analysis, and writing the paper. CB, as the PhD supervisor, provided oversight, theoretical support, and guidance in refining the research methodology and paper.

Competing interests. Tahir H. Malik's PhD was funded by Vattenfall, where he is also employed. The authors have no other competing interests to declare.

Disclaimer. Publisher's note: Copernicus Publications remains neutral with regard to jurisdictional claims made in the text, published maps, institutional affiliations, or any other geographical representation in this paper. While Copernicus Publications makes every effort to include appropriate place names, the final responsibility lies with the authors.

Acknowledgements. The support of Vattenfall, particularly for financing this study and providing access to vital wind turbine resources, is gratefully acknowledged. The use of an AI language model, OpenAI (2024), is also acknowledged for refining a previous version of the paper.

Review statement. This paper was edited by Alessandro Bianchini and reviewed by three anonymous referees.

References

Abolude, A. T. and Zhou, W.: Assessment and Performance Evaluation of a Wind Turbine Power Output, Energies, 11, 992, https://doi.org/10.3390/en11081992, 2018.

Badihi, H., Zhang, Y., Jiang, B., Pillay, P., and Rakheja, S.: A comprehensive review on signal-based and model-based condition monitoring of wind turbines: Fault diagnosis and lifetime prognosis, P. IEEE, 110, 754–806, https://doi.org/10.1109/JPROC.2022.3171691, 2022.

Bak, C.: Aerodynamic design of wind turbine rotors, Advances in wind turbine blade design and materials, Second edition, edited by: Brøndsted, P., Nijssen, R., and Goutianos, S., Woodhead Publishing, Elsevier, https://doi.org/10.1016/B978-0-08-103007-3.00001-X, 2023.

Bak, C., Zahle, F., Bitsche, R., Kim, T., Yde, A., Henriksen, L., Hansen, M., Blasques, J., Gaunaa, M., and Natarajan, A.: The DTU 10-MW Reference Wind Turbine, danish Wind Power Research 2013, 27–28 May 2013, https://orbit.dtu.dk/en/publications/the-dtu-10-mw-reference-wind-turbine (last access: 27 March 2024), 2013.

Bak, C., Skrzypiński, W., Gaunaa, M., Villanueva, H., Brønnum, N. F., and Kruse, E. K.: Full scale wind turbine test of vortex generators mounted on the entire blade, J. Phys. Conf. Ser., 753, 022001, https://doi.org/10.1088/1742-6596/753/2/022001, 2016.

Bak, C., Forsting, A. M., and Sorensen, N. N.: The influence of leading edge roughness, rotor control and wind climate on the loss in energy production, J. Phys. Conf. Ser., 1618, 052050, https://doi.org/10.1088/1742-6596/1618/5/052050, 2020.

Bak, C., Olsen, A., Forsting, A., Bjerge, M., Handberg, M., and Shkalov, H.: Wind tunnel test of airfoil with erosion and leading edge protection, J. Phys. Conf. Ser., 2507, https://doi.org/10.1088/1742-6596/2507/1/012022, 2023.

Bak, D., Andersen, P., Madsen Aagaard, H., Gaunaa, M., Fuglsang, P., and Bove, S.: Design and verification of airfoils resistant to surface contamination and turbulence intensity, in: Collection of Technical Papers – AIAA Applied Aerodynamics Conference, AIAA 2008–7050, American Institute of Aeronautics and Astronautics, 26th Applied Aerodynamics Conference, 18–21 August 2008, https://doi.org/10.2514/6.2008-7050, 2008.

Barthelmie, R. J. and Jensen, L.: Evaluation of wind farm efficiency and wind turbine wakes at the Nysted offshore wind farm, Wind Energy, 13, 573–586, https://doi.org/10.1002/we.408, 2010.

Cappugi, L., Castorrini, A., Bonfiglioli, A., Minisci, E., and Campobasso, M. S.: Machine learning-enabled prediction of wind turbine energy yield losses due to general blade leading edge erosion, Energ. Convers. Manage., 245, 114567, https://doi.org/10.1016/j.enconman.2021.114567, 2021.

Castorrini, A., Ortolani, A., and Campobasso, M. S.: Assessing the progression of wind turbine energy yield losses due to blade erosion by resolving damage geometries from lab tests and field observations, Renew. Energ., 218, 119256, https://doi.org/10.1016/j.renene.2023.119256, 2023.

Ding, Y., Barber, S., and Hammer, F.: Data-Driven wind turbine performance assessment and quantification using SCADA data and field measurements, Frontiers in Energy Research, 10, 1050342, https://doi.org/10.3389/fenrg.2022.1050342, 2022.

Do, M.-T. and Berthaut-Gerentes, J.: Optimal time step of SCADA data for the power curve of wind turbine, J.

Phys. Conf. Ser., 1102, 012025, https://doi.org/10.1088/1742-6596/1102/1/012025, 2018.

Ehrmann, R. S., Wilcox, B., White, E. B., and Maniaci, D. C.: Effect of surface roughness on wind turbine performance, Tech. rep., Sandia National Lab.(SNL-NM), Albuquerque, NM, United States, https://doi.org/10.2172/1596202, 2017.

Elliott, D. and Infield, D.: An assessment of the impact of reduced averaging time on small wind turbine power curves, energy capture predictions and turbulence intensity measurements, Wind Energy, 17, 337–342, https://doi.org/10.1002/we.1579, 2012.

EMD International A/S: WindPRO Software for Wind Energy Analysis, https://www.emd.dk/windpro/ (last access: 1 June 2023), 2023.

Gaudern, N.: A practical study of the aerodynamic impact of wind turbine blade leading edge erosion, J. Phys. Conf. Ser., 524, 012031, https://doi.org/10.1088/1742-6596/524/1/012031, 2014.

Gonzalez, E., Stephen, B., Infield, D., and Melero, J. J.: On the use of high-frequency SCADA data for improved wind turbine performance monitoring, J. Phys. Conf. Ser., 926, 012009, https://doi.org/10.1088/1742-6596/926/1/012009, 2017.

Gonzalez, E., Stephen, B., Infield, D., and Melero, J. J.: Using high-frequency SCADA data for wind turbine performance monitoring: A sensitivity study, Renew. Energ., 131, 841–853, 2019.

Han, W., Kim, J., and Kim, B.: Effects of contamination and erosion at the leading edge of blade tip airfoils on the annual energy production of wind turbines, Renew. Energ., 115, 817–823, https://doi.org/10.1016/j.renene.2017.09.002, 2018.

Hansen, M. O.: Aerodynamics of wind turbines, Earthscan, James & James, 8, 14, Earthscan Ltd, ISBN 978-1844074389, 2008.

International Electrotechnical Commission (IEC): Wind turbines – Part 1: Wind turbine generators – General requirements, Tech. rep., Geneva, Switzerland, https://webstore.iec.ch/en/publication/26423 (last access: 27 March 2024), 2019.

Jonkman, J., Butterfield, S., Musial, W., and Scott, G.: Definition of a 5-MW Reference Wind Turbine for Offshore System Development, https://doi.org/10.2172/947422, 2009.

Kim, D.-Y., Kim, Y.-H., and Kim, B.-S.: Changes in wind turbine power characteristics and annual energy production due to atmospheric stability, turbulence intensity, and wind shear, Energy, 214, 119051, https://doi.org/10.1016/j.energy.2020.119051, 2021.

Krog Kruse, E., Bak, C., and Olsen, A. S.: Wind tunnel experiments on a NACA 633-418 airfoil with different types of leading edge roughness, Wind Energy, 24, 1263–1274, https://doi.org/10.1002/we.2630, 2021.

Kruse, E.: A Method for Quantifying Wind Turbine Leading Edge Roughness and its Influence on Energy Production: LER2AEP, Phd, DTU Wind Energy, Roskilde, Denmark, (DTU Wind Energy PhD), https://orbit.dtu.dk/en/publications/a-method-for-quantifying-wind-turbine-leading-edge-roughness-and–2 (last access: 27 March 2024), 2019.

Larsen, T. J. and Hansen, A. M.: How 2 HAWC2, the user's manual, Risø National Laboratory, https://orbit.dtu.dk/en/publications/how-2-hawc2-the-users-manual (last access: 27 March 2024), 2007.

Malik, T. H. and Bak, C.: Full-scale wind turbine performance assessment using the turbine performance integral (TPI) method: a study of aerodynamic degradation and operational influences, Wind Energ. Sci., 9, 2017–2037, https://doi.org/10.5194/wes-9-2017-2024, 2024.

Maniaci, D., White, E., Wilcox, B., Langel, C., van Dam, C., and Paquette, J.: Experimental Measurement and CFD Model Development of Thick Wind Turbine Airfoils with Leading Edge Erosion, J. Phys. Conf. Ser.,753, 022013,, https://doi.org/10.1088/1742-6596/753/2/022013, 2016.

Mann, J.: The spatial structure of neutral atmospheric surface-layer turbulence, J. Fluid Mech., 273, 141–168, 1994.

OpenAI: ChatGPT: Optimizing Language Models for Dialogue, https://openai.com/chatgpt/ (last access: 28 November 2024), 2024.

Saint-Drenan, Y.-M., Besseau, R., Jansen, M., Staffell, I., Troccoli, A., Dubus, L., Schmidt, J., Gruber, K., Simões, S. G., and Heier, S.: A parametric model for wind turbine power curves incorporating environmental conditions, Renew. Energ., 157, 754–768, https://doi.org/10.1016/j.renene.2020.04.123, 2020.

Skrzypinski, W., Gaunaa, M., and Bak, C.: The Effect of Mounting Vortex Generators on the DTU 10MW Reference Wind Turbine Blade, vol. 524, IOP Publishing, 5th International Conference on The Science of Making Torque from Wind 2014, TORQUE 2014, 10–20 June 2014, https://doi.org/10.1088/1742-6596/524/1/012034, 2014.

St. Martin, C. M., Lundquist, J. K., Clifton, A., Poulos, G. S., and Schreck, S. J.: Wind turbine power production and annual energy production depend on atmospheric stability and turbulence, Wind Energ. Sci., 1, 221–236, https://doi.org/10.5194/wes-1-221-2016, 2016.

Wagner, R., Courtney, M., Larsen, T. J., and Paulsen, U. S.: Simulation of shear and turbulence impact on wind turbine performance, Danmarks Tekniske Universitet, Risø Nationallaboratoriet for Bæredygtig Energi, https://orbit.dtu.dk/en/publications/simulation-of-shear-and-turbulence-impact-on-wind-turbine-perform (last access: 27 March 2024), 2010.

Wharton, S. and Lundquist, J. K.: Atmospheric stability affects wind turbine power collection, Environ. Res. Lett., 7, 014005, https://doi.org/10.1088/1748-9326/7/1/014005, 2012.

Yang, W., Tavner, P. J., Crabtree, C. J., Feng, Y., and Qiu, Y.: Wind turbine condition monitoring: technical and commercial challenges, Wind Energy, 17, 673–693, https://doi.org/10.1002/we.1508, 2014.